Basin Research (2004) **16**, 413–430, doi: 10.1111/j.1365-2117.2004.00239.x

Detrital thermochronology – a new perspective on hinterland tectonics, an example from the Andean Amazon Basin, Ecuador

G. M. H. Ruiz,* D. Seward and W. Winkler

Geology Institute, ETH Zentrum, Zurich, Switzerland
**Present address: FALW, Department of Isotope Geochemistry, HV Amsterdam, The Netherlands*

ABSTRACT

In order to understand the significance of detrital grain ages in sedimentary basins, a new approach is presented. Five characteristic paths, identified by the change in age of detrital grain populations combined with the change in lagtime over time, can be related to different geodynamic settings in the source regions. When lagtime and grain age increase over time, a change in source must be invoked – this is usually a direct response to a geological event. A constant cooling age, a vertical path, associated implicitly with increasing lagtime, implies erosion of materials that had passed through the closure temperature rapidly – exhuming sufficient rock to supply detritus over the time of the path. Constant lagtimes, regardless of the lagtime itself, are indicative of thermochronological stability in the source region. This can involve fast or slow cooling. Finally, decreasing lagtimes support the notion of increasing cooling rates in the source regions over time. A test study is presented from sediments of the northern Ecuadorian Sub-Andean Zone where geological events had previously been identified using alternative methods. The addition of heavy-mineral studies increased the precision in the interpretation. At 90 Ma, rapidly decreasing lagtimes point to a phase of tectonic activity. From about 85 Ma until about 60 Ma the lagtimes were approximately zero. This represents a phase of rapid exhumation of the source regions correlating with the previously identified Pallatanga event. An associated increase of metamorphic minerals occurs over this time span, pointing to increased erosion from deeper horizons. At about 70 Ma, the oldest source region, the shield to the east, was switched off. This timing correlates with a change from marine to continental conditions in the basin, a change in palaeocurrent directions from the east to the west, as well as an associated influx of material from the growing Cordillera Real. At about 55 Ma, a change in source is identified by a change in slope of the lagtime curve together with a change in heavy minerals. From 50 to 35 Ma a renewed period of tectonism in the source region is correlated with the docking of the Macuchi terrane which clearly had an effect of increased erosion in the Cordillera Real bringing in higher grade metamorphic minerals. From about 32 Ma onwards the lagtime has been somewhat constant at about 30 Myr. This does not imply, however, a steady-state environment as it is well known from other geological evidence that there have been other events within this time frame. One must be cautious about over-interpreting the lagtime as a method to determine steady state in any region. It is a matter of scale.

INTRODUCTION

Siliclastic sediments generally contain grains derived from a number of sources. Hence, the varied thermal histories experienced in the source regions will be reflected in the distribution of the cooling ages recorded in the detrital grains of the sedimentary basin (Naeser, 1979). The source region has by definition been eroded but the thermal history which it had experienced can still be gauged through the detrital thermochronology of minerals within the sediments.

Thermochronometers that are particularly sensitive to the movement of rocks through the uppermost crust are those of the fission-track system because their effective closure temperatures range from $\sim$260 to $\sim$120 °C for zircon and apatite, respectively (Green *et al.*, 1989; Brandon *et al.*, 1998). Many previous basin studies have been carried out using these chronometers (e.g. Hurford *et al.*, 1984; Zeitler *et al.*, 1986; Cerveny *et al.*, 1988; Hurford & Carter, 1991; Brandon & Vance, 1992; von Eynatten *et al.*, 1996; Najman *et al.*, 1997; Carter, 1999; Carter & Moss, 1999;

Correspondence: G. M. H. Ruiz, FALW, Department of Isotope Geochemistry, De Boelelaan 1085, 1081 HV Amsterdam, The Netherlands. E-mail: ruig@geo.vu.nl

Garver *et al*., 1999; Spiegel *et al*., 2000; Bernet *et al*., 2001) but have not taken the interpretative and long-term approach discussed here.

The purpose of this paper is to present some essential definitions and concepts regarding detrital thermochronology and to derive a theoretical model that can be used to determine the long-term exhumation histories of source regions and their geodynamic implications. This model has then been applied to the northern retro-foreland fold and thrust belt (hereon referred to as the Sub-Andean Zone (SAZ)) of the Ecuadorian Andes, utilising a series of zircon fission-track (ZFT) data from detrital grains and heavy-mineral analysis, extracted from Middle Cretaceous – Recent siliciclastic sedimentary rocks. The SAZ is a suitable region to test the applicability of the model, because it preserves a long reasonably continuous history of sedimentation (Cretaceous – Recent, Tschopp, 1953), exposed within a fold and thrust belt system to the west of the flat-lying Andean Amazon Basin (AAB) or Oriente region. In addition, previous studies have established a detailed spatial pattern of exhumation histories for various regions of the Ecuadorian Andes (Litherland *et al*., 1994; Jaillard *et al*., 1997; Pecora *et al*., 1999; Rivadeneira & Baby, 1999; Spikings *et al*., 2000, 2001; Hughes & Pilatasig, 2002; Kerr *et al*., 2002; Christophoul *et al*., 2002a), which can be used as an independent test for the model.

DETRITAL THERMOCHRONOLOGY

Any mineral phase associated with a radiometric-based, geochronological technique may be implemented for detrital thermochronology, assuming that the single grain ages have not undergone any resetting as they were deposited. The temperature of resetting depends on the closure temperature of the particular decay chain being analysed. Several techniques, such as vitrinite reflectance (Burnham & Sweeney, 1989; Barker, 1996) and illite crystallinity (Blenkinsop, 1988) have traditionally been used to determine maximum palaeo-temperatures attained in a basin during burial, although they do not provide any temporal information. Apatite fission-track (AFT) analysis records events that have taken place at temperatures lower than approximately 120 °C. Modelling of the AFT data sets (e.g. Gallagher, 1995) can potentially reveal plausible thermal history solutions within the temperature range of 120–60 °C. AFT analysis can be applied to both the sedimentary rocks and the underlying basement. Additionally, one of the most useful minerals in detrital grain age studies is zircon, which can also be treated using the same method. Zircon is usually abundant in siliciclastic sediments because of its resistance to mechanical and chemical alteration during transport and diagenesis. Wide-ranging values for the temperature sensitivity of fission tracks in zircon have been published (e.g. Yamada *et al*., 1995; Tagami *et al*., 1996; Brandon *et al*., 1998). Most of the zircons analysed in this study host significant α damage and therefore we have chosen to implement the closure temperature of Brandon *et al*. (1998), which ranges from ≈260 to 215 °C for cooling rates of 100 to 1 °C Myr^{-1}, respectively.

A combination of different methods allows the accuracy of interpretation to be increased. For example, recent studies of the exhumation of the Alpine orogeny combined detrital thermochronology with lithological observations on pebbles (Dunkl *et al*., 1998; Spiegel *et al*., 2000; Brügel *et al*., 2003). Carter & Moss (1999) suggested that the method could be improved by the use of U/Pb dating on the zircon grains from the same suites. Later, however, Carter & Bristow (2003) concluded that the better regional information is yielded from the fission-track system and that the U/Pb system may not be necessarily source exclusive. An excellent review of the literature and applications is presented in Brewer *et al*. (2003) who also applied modelling to detrital $^{40}Ar/^{39}Ar$ ages derived from the Himalayas.

Lagtime concept

Using ZFT, Zeitler *et al*. (1986) and Cerveny *et al*. (1988) first used the concept of lagtime in a study of the Neogene molasse-type sediments in northern Pakistan whose source rocks were the growing Himalayas. The lagtime (L_g) is defined as the difference between the time of closure of the geochronological system in the source region and time of deposition in the basin (Fig. 1).

From any sample, the different detrital age populations can statistically be extracted from raw data (Sambridge & Compston, 1994; Brandon, 1996) and classified in increasing ages from $P_1, P_2, \ldots, P_n$, where P_1 is the youngest population and P_n the oldest (Garver *et al*., 1999; Bernet *et al*., 2001). Each detrital population P_n is characterised by its cooling age (t_{c_i}) and by the stratigraphic (or depositional) age of the sediment from which it was extracted (t_{d_i}) (Fig. 1). Thus $L_{g_i} = t_{c_i} - t_{d_i}$ (Fig. 1). Short lagtimes reflect tectonic activity and rapid erosion in the source regions whereas long lagtimes may suggest that the source regions underwent very slow exhumation as passing through T_c (Fig. 1). The latter may also include cannibalistic erosion of non-reset sediments, i.e. recycling, hence time between first deposition and redeposition may not be negligible ($t_e - t_d \neq 0$; Fig. 1), and as a consequence, syn-orogenic exhumation rates cannot be constrained. Long lagtime scenarios may also include more rapid pulses hidden above T_c (Fig. 1). This can be considered as the removal of the 'thermochronological dead' zone, a zone with ages reflecting an earlier thermal history. At the onset of any orogenic phase, the cover rocks, the dead layer, must first be eroded before syn-orogenic exhumation can be estimated. Once denudation has reached such levels, then it is possible to estimate the exhumation rate in the source region by dividing the estimated depth of closure (Z_c) by the lagtime (L_g): $E \times h = Z_c/L_g$ in mm yr^{-1} (Garver *et al*., 1999), on the assumption that the time of transport from erosion site to basin is negligible ($t_e - t_d = 0$; Fig. 1). This clearly suggests that both the calculation of exhumation rates using detrital grain ages, and the time of onset of an orogenic phase should always be treated with care.

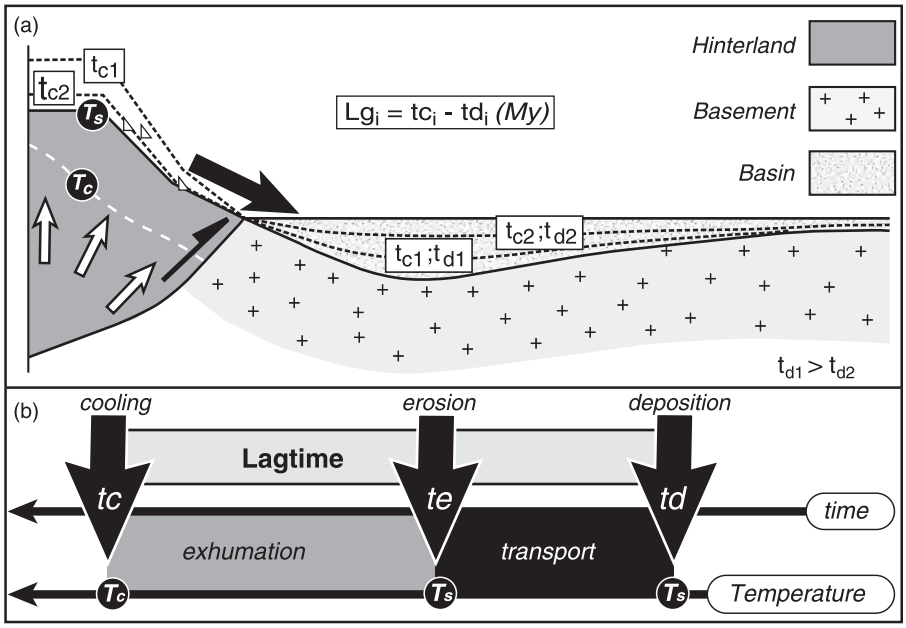

Fig. 1. The notion of lagtime as described by Zeitler *et al.* (1986) in (a) a schematic cross-section and (b) within time temperature scales. The lagtime includes the time taken for the mineral to cool through the specific closure temperature, T_c, to the surface where the temperature is T_s and transported into the basin. The times of closure, exposure on the surface and time of deposition (stratigraphic age) are t_c, t_e and t_d, respectively. t_{c1} and t_{c2} represent two levels in the hinterland that were denuded and carried into the basin where the respective stratigraphic ages are t_{d1} and t_{d2}.

The present study emphasises the concept of lagtime as it changes temporally, and attempts to use these changes as an indicator of orogenic activity in the hinterland, with special reference to the Ecuadorian Andes. But first some assumptions must be outlined.

(a) The lagtime of detrital grains must be zero or positive; $Lg_i \geq 0$. If not, this indicates that the rock has undergone temperatures higher than the closure temperature of the mineral in question since deposition and therefore information regarding the exhumation of the source region has been lost. It may also imply that the stratigraphic age is not well constrained.

(b) The first rocks exhumed to the surface in a thermally homogenous block, have older ages than those below ($t_{c1} > t_{c2}$; Fig. 1). Thus, detrital ages younging upwards is the normal pattern expected from a single eroding tectonic block (Garver *et al.*, 1999). It will be shown, however, that this is not always the case.

(c) Possible contemporaneous volcanic contamination generates zero lagtime as deposition is instantaneous, and the ages lies on the 1 : 1 line (Fig. 2). Such input can be checked by examination of the lithological and mineralogical properties of the sediment and must be excluded from any interpretation of hinterland exhumation rates because it would otherwise misleadingly imply very high rates.

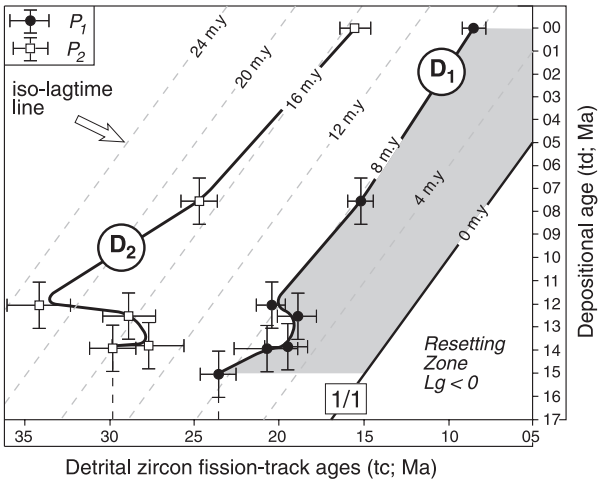

Fig. 2. Detrital zircon fission-track data set for middle Miocene to Recent levels of the Ligurid–Appenines basin (adapted after Bernet *et al.*, 2001). Error bars are ± 1 standard error for FT ages and ± 1 Ma uncertainty for depositional ages. Almost all sites yield two detrital age populations that are plotted against the stratigraphic ages of the hosting sediments. The age populations are joined together per rank, generating the D_1 and D_2 curves. The 1 : 1 line represents a zero lagtime line. Any grains to the right of this line must have been reset during burial ($L_g < 0$) or the site has an erroneous stratigraphic age. Zero lagtime is an indicator of either excessively fast source denudation or volcanic input. The latter can be identified usually through heavy mineral content. The variation of the lagtime up-sequence along the D_1 curve is shaded in dark grey.

PROPOSED METHODOLOGY

As discussed above, age populations are extracted for each stratigraphic horizon and classified in increasing order from P_1, P_2, . . ., P_n. These ages are then plotted against the stratigraphic age to determine any temporal trends (Fig. 2). Such procedures have been employed in recent

publications (e.g. Carter, 1999; Garver *et al.*, 1999; Bernet *et al.*, 2001; Carrapa *et al.*, 2003; Najman *et al.*, 2003). Added to these plots is the 1 : 1 line, which is the graphical representation of detrital grain age populations equal to the stratigraphic age ($t_{c_i} = t_{d_i}$), a zero lagtime line. A clear advantage of this sort of plot is the immediate visual assessment of the lagtime variability and the identification of ages lying in the zone of resetting.

Detrital D_n curves

In order to visualise the change in the lagtime upwards in the section, the detrital age populations, ranked as P_1 to P_n, are linked together generating the D_1 to D_n curves (Fig. 2). This does not necessarily imply that the populations, which constitute any particular D_i curve, are genitically related or always share the same provenance. Rather, this is solely a graphical approach to examine the relative temporal changes in cooling and exhumation rate in the source regions. Furthermore, the variation in heavy-mineral assemblages can be used to bolster or dispute the theoretical interpretation of distinct changes in lagtime along the D_i curve. The D_1 curve hosts the population with the shortest lagtime and consequently, the most probable record of rapid episodes of hinterland cooling. It is the easiest to interpret with confidence – it is less likely to have been through several cycles of erosion and deposition. Moreover, the oldest populations may be missing in the ZFT system because of the fact that the track density is too great to be counted (Garver *et al.*, 1999). Inflexion points along a D_n curve may indicate some change in the exhumation of the source region but an inflexion point alone does not constrain the timing of the event, it is only an indication that an event has occurred. The event most likely took place earlier and it was not recorded immediately at the surface. Hence, each situation must be carefully considered in its own right. Any extensive detrital curve is composed of successive paths that are best considered in their simplest forms, i.e. as lines. When studying long segments with many data points, and considering uncertainties on both ages (t_c and t_d), a regression line may specify the appropriate (a; b) values for each segment as described in Bernet *et al.* (2001):

$$t_c = f(t_d) \quad \text{with } t_c = a \times t_d + b$$
$$as\ L_g = t_c t_d\ (1) \ \Leftrightarrow L_g = (a-1) \times td + b.$$

Paths

Detrital ages vary upwards within the stratigraphic column with conspicuous paterns – we present here the various possible paths that may be observed along the D_n curves. An infinite number of paths are possible, but in realistic terms five have been identified (Fig. 3). They are characterised on the basis of upward variation in both the lagtime (L_g) and the thermochronological detrital age (t_c).

Type 1 path [0–1] [$a < 0$; b] 'older ages upwards' (Fig. 3)

In a type 1 path the detrital ages and the lagtime increase upwards in the stratigraphic sequence (Fig. 3) – yielding a negative gradient. Various geological scenarios might be cited for such a pathway. (a) Erosion of a non-reset volcanic sequence with older ages at the base. Such a scenario can be checked by the heavy-mineral contribution to the basin. (b) The cannibalisation of non-reset sediments, which themselves had the normal younging upward cycle is another example. Erosion of 'older' deposits is frequent

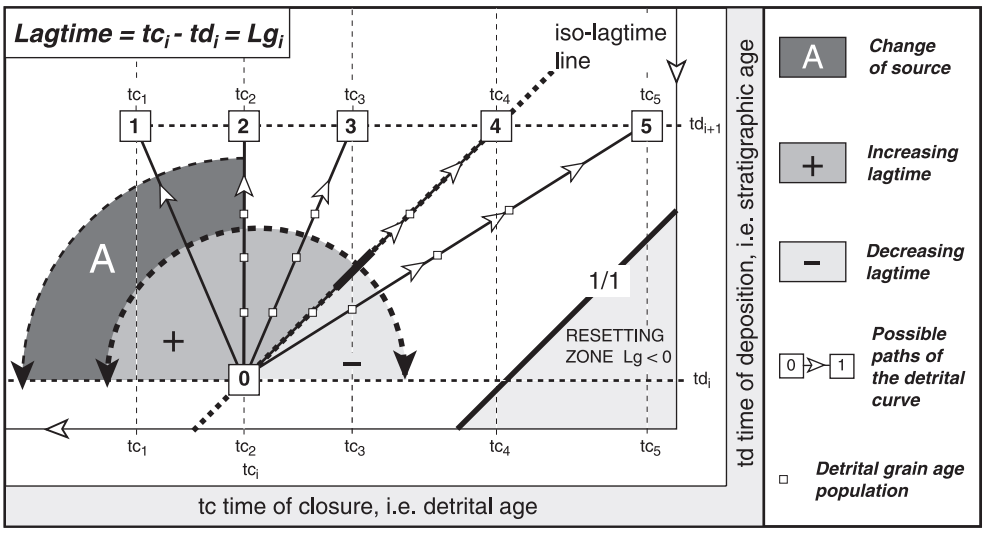

Fig. 3. Possible paths upwards along a detrital curve D_n. Five paths are defined on the basis of variation in lagtime (L_g) and time of closure (t_c). 0 $[t_{c_i}; t_{d_i}]$ is the starting point of all the paths that have the same incrementation within the stratigraphic column ($t_{d_{i+1}}$) to facilitate comparison. The y-axis represents the depositional age (t_d) of the hosting sediment whereas the x-axis is the thermochronological age of the detrital population (t_c). Note the directions of both axes, particularly the y-axis which corresponds to a younging upward direction in the stratigraphic column.

during any phase of orogenesis. Such sediments may be cannibalised from within or reworked from outside the basin. (c) A major change in hinterland tectonics will have an effect on the drainage systems, bringing into the system source rocks which are probably different and inherited, at least at the beginning thermochronological ages. All three scenarios correspond to sourcing from the 'thermochronologically dead' zone (see above), and as a result no exhumation rate can be estimated for the tectonic change in question from these early deposits. Finally, the timing of the inferred change of provenance is dated by the change towards a negative gradient $t_{di} > t > t_{di}$ (Fig. 3).

Type 2 path [0–2] [a = 0; b] 'constant time of closure' (Fig. 3)

Type 2 path is characterised by a constant cooling age (t_c; Fig. 3) upwards in the stratigraphic column and hence requires the erosion of source(s) with a homogenous '*b*' million-year cooling age. The erosion of sequences with constant time of closure may include (thick) piles of volcanics that were rapidly extruded over short time periods, e.g. plateau basalts, but also rapidly quenched blocks over large regions. This latter may be exemplified in the study of Garver & Brandon (1994) from the Coast Plutonic Complex of southern British Colombia. It has also recently been reported by Carrapa *et al*. (2003) who determined $^{40}Ar/^{39}Ar$ ages on detrital white micas from the sediments of the Tertiary Piedmont Basin (Italy). These authors suggest that a period of very fast cooling prior to 38 Ma was able to produce sufficient crustal material with a relative uniform age signature to supply > 30 Myr of erosion products into the basin. Very old populations, which were derived from a source region, such as a craton, with low denudation may also yield this path because of their large error bars.

Type 3 path [0–3] [0 < a < 1; b] 'increasing lagtime with positive gradient' (Fig. 3)

Ages decreasing upwards (Fig. 3), but with increasing lagtime, are the characteristic pattern of type 3 paths. Such a path represents abatement of the exhumation rate assuming a constant depth of closure. On the other hand, it could represent a relaxation of the geotherms and a fall in the geothermal gradient. Both scenarios are events that might follow an orogenic pulse.

Type 4 path [0–4] [a = 1; b] 'constant lagtime' (Fig. 3)

A constant lagtime through the stratigraphic record is indicated by an alignment of the detrital grain age populations along an iso-lagtime line (Bernet *et al*., 2001) with $L_g = b$, and $a = 1$ (Fig. 3). A constant lagtime upward in the stratigraphic column indicates that an invariant time was necessary to bring rocks to the surface and hence, cooling in the source region(s) remained at a constant mean rate during a period of time equal to the lagtime for the duration of this record [t_{c_i}; t_{c4}] (Fig. 3), considering T_c and T_s constant over time. Consequently, a type 4 path characterises a 'steady-state of cooling' or 'thermochronological steady-state' within the source region, which started prior to the age of the oldest population along that path. Such a path does not necessarily imply that the hinterland underwent a 'steady-state exhumation' (Bernet *et al*., 2001), i.e. the absence of surface uplift (England & Molnar, 1990). For instance, a rapid and steady-state phase of exhumation in source regions would generate high cooling rates as denudation permits the isotherms to move closer to the surface (Moore & England, 2001). As a result, decreasing lagtimes (type 5 path) would be logically expected in the sourced basin(s). A steady state of exhumation is believed to characterise developed orogens (Willet & Brandon, 2002), after the 'dead' zone has been removed and before the orogen goes into a decay phase (Garver *et al*., 1999), which would be typified by longer lagtimes.

A constant lagtime, approaching zero, is a record of persistent and extremely rapid cooling that can be directly related to very rapid exhumation in the hinterland, assuming that contemporaneous and continuous volcanic contamination can be excluded. Examples of source regions that may be supplying such young ages are the syntaxes of the Himalayas, where ZFT ages are less than 0.5 Ma (Seward and Burg, 2004, pers. comm.). A type 4 path with a small *b* value of ~8 Myr was produced from the Ligurid–Apennines Basin (Fig. 2, Bernet *et al*., 2001) that probably points towards a single phase of exhumation in the developed Alpine orogen.

What is the significance when long lagtimes, e.g. ~30 Myr, persist for an extended period? The simplest explanation is that exhumation proceeded in the hinterland at a low and constant rate (within uncertainties) for a long period (Garver & Brandon, 1994). An alternative is that two deferred and short-lived phases of exhumation affected the same source region at the same rate, the second one forcing to the surface the rocks that were previously cooled through T_c by the first phase.

Type 5 path [0–5] [a > 1; b] 'decreasing lag time' (Fig. 3)

Type 5 path is characterised by a decreasing lagtime upsection which implies increasing cooling rates (Garver *et al*., 1999) in the source region. This is the orogenic growth phase. Dividing the estimated depth of closure (Z_c) by the time needed for the last population along the path to reach the surface (L_g), and considering a negligible transport time ($t_d - t_e = 0$; Fig. 1), brings an estimation of the maximum value of the exhumation rate in the hinterland for the considered period: $Exh = Z_c/L_g$ in mm yr^{-1} (Garver *et al*., 1999).

Common trends

Noticeably, the commonality of the trends of the D_n curves is sometimes quite remarkable and may have important regional implications. Let us consider a region made up of various blocks/units that had undergone different thermal cooling (Fig. 4) such that at the surface different cooling

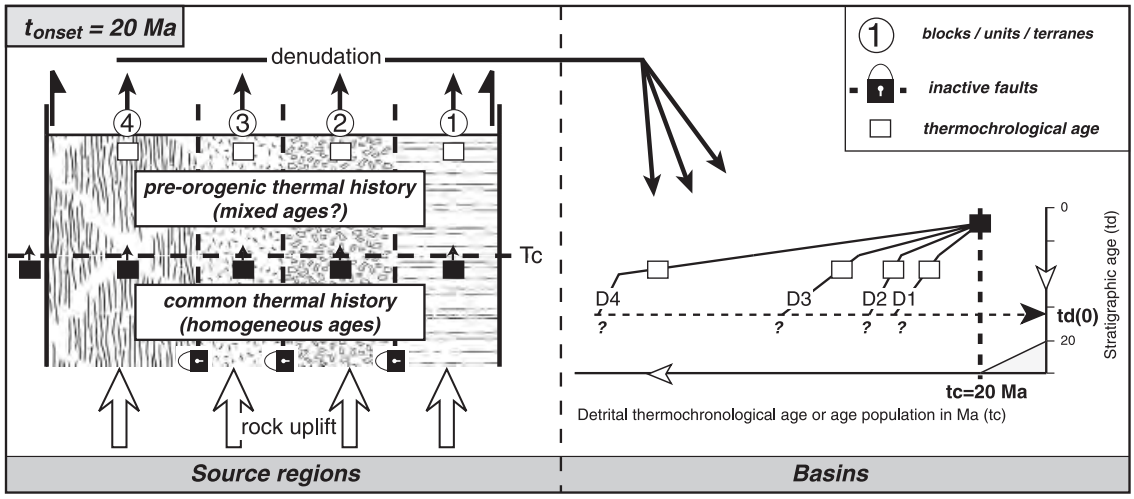

Fig. 4. Common trends for the D_n curves. Parallel to sub-parallel n detrital curves in the basins are probably derived from n commonly cooling exhuming sources that previously underwent different cooling histories. The D_n curves will converge, once the pre-orogenic thermal history is removed into a point that defines the onset (t_c = 20 Ma in this case) of the renewed exhumational phase. This can be used to identify events (tectonic and/or thermal, etc.) in the hinterland.

ages were exposed. The erosion of this heterogeneous source region would firstly yield different detrital thermochronological curves into the basin, each individual curve being derived from one block/unit. Once the 'thermochronologically dead' layer has been removed/eroded, all the curves should finally merge to one point, e.g. t_c = 20 Ma (Fig. 4). This point corresponds approximately to the timing of the renewed/common pulse.

An example of common trends is the two parallel ZFT detrital D_1 and D_2 curves with constant lagtimes of, respectively, 8 and 15 Myr from the Middle Miocene to Recent deposits of the Appenines Basin (Fig. 2; Bernet *et al*., 2001). The authors suggested that the two source regions are possibly the hanging wall and footwall of the active normal Simplon Fault from the Central Alps, whereas the offset in ages of the populations (~7 Myr) is related to differential exhumation across the fault (Sooms, 1990). When did this start? As already discussed above, a minimum age for the onset of this phase responsible for such characteristic type 4 paths is indicated by the age (t_c) of the first population along this path, i.e. 23 Ma considering the D_1 curve, whereas an older age of 30 Ma (Fig. 2) is suggested by the D_2 curve. It is therefore conceivable that differential exhumation developed at least 30 Myr ago in the hinterland of the Appeninic Basin. The first syn-orogenic deposits of Middle Oligocene age would have probably yielded ZFT populations with inherited thermal history before syn-tectonic cooling ages appeared in the basin by the Miocene as evidenced by Bernet *et al*., (2001).

AN EXAMPLE FROM THE ANDEAN AMAZON BASIN, ECUADOR

The northern Andes are the product of the subduction of the oceanic Nazca plate beneath the western edge of the South American plate (Fig. 5). In Ecuador, the double vergent orogenic belt comprises deformed metamorphosed continental margin series including various plutons (Cordillera Real; Litherland *et al*., 1994) and oceanic plateau and volcanic arc units that were accreted during Late Cretaceous and Early Tertiary times (Cordillera Occidental and Costa; Jaillard *et al*., 1997; Hughes & Pilatasig, 2002). During this time, to the east of the orogen, the Andean Amazon Basin (AAB) developed in a retro-arc foreland position (Christophoul *et al*., 2002a, b) even though only minor thrusting of the Guyana Shield is evident (Fig. 5). According to many authors (Tschopp, 1953; Baldock, 1982; Balkwill *et al*., 1995; Jaillard, 1997; Christophoul, 1999; Rivadeneira & Baby, 1999), the main derivation of the AAB switched by the Late Cretaceous with the deposition of Tena Fm. from Shield regions located to the east (Fig. 5) to the rising Andes to the west (Fig. 5). The Aptian to Recent basin fill series of the AAB and their Jurassic magmatic basement, i.e. the Misahualli Fm. and Abitagua batholith (Wasson & Sinclair, 1927; Colony & Sinclair, 1932), crop out in the SAZ (Fig. 6). Their maximum sedimentary thickness further to the east, in the flat-lying Oriente region (Tschopp, 1953; Christophoul, 1999) ranges between ~3350 and 1600 m. The sediments are dominantly clastic, and deposited in fluvial environments with the exception of the Napo and Orteguaza deposits (Jaillard, 1997; Christophoul *et al*., 2002b).

As an initial study, AFT analysis was applied to samples from the basement rocks, in order to constrain whether the basement had been above 120 °C, i.e. closure of the apatite system (Green *et al*., 1989). At all sites, except those very close to faults, apatite ages range from 183 to 116 Ma and their modelled thermal histories reveal that they were never over 120 °C (Ruiz, 2002). This therefore implies that ZFT ages from the sedimentary cover, with a higher closure temperature (260–215 °C; Brandon *et al*., 1998), have not lost provenance information and allows the exhumation of the hinterland to be investigated from Aptian to Recent times.

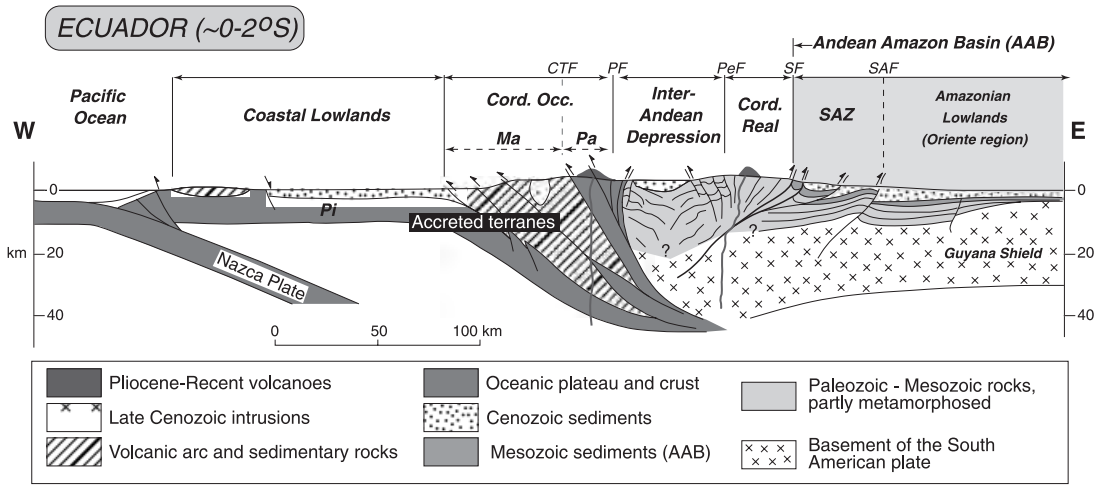

Fig. 5. Cross-section through the Ecuadorian Andes at latitude 2°S (modified after Jaillard *et al.*, 2002b). The northern Ecuadorian Sub-Andean Zone (SAZ) defines the western and exhumed margin of the Ecuadorian Amazon Basin (AAB). It is bounded to the east by the Sub-Andean front (SAF) and to the west by the Sub-Andean Fault (SF). Pi, Ma, Pa: Pinon, Macuchi and Pallatanga terranes. CTF, Pf, PeF: Chimbo–Toarchi Fault, Pujuli-Pallatanga Fault, Peltetec Fault. Cord. Occ: Cordillera Occidental.

Methods

Up to 24 sedimentary rocks, ranging from Aptian to Recent were sampled from the proximal deposits preserved in the SAZ (Fig. 6). Lithologies vary from conglomerates to sandstones and a few siltstones. Large representative samples (> 5 kg) were separated in order not to bias potential provenance information. The various zircon populations were split by size and magnetic susceptibility. Because etching time of zircons for fission-track is proportional to the radiation damage (Naeser, 1979; Cerveny *et al.*, 1988), zircon mounts from the same sample (up to eight) were etched in a eutectic melt of NaOH–KOH at 210 °C (Gleadow *et al.*, 1976) with 1-h increments. The more highly damaged zircons required only a short etch time of the order of 3 h, whereas less damaged crystals were etched longer to reveal fission tracks. Samples were irradiated at the ANSTO facility, Lucas Heights, Australia. Zircons were counted at a magnification of ×1600 (oil). All ages were calculated using the zeta approach (Hurford & Green, 1983) combining the age standards, Fish Canyon Tuff with dosimeter glass CN1, yielding a ζ value of 121 ± 3. Fifty zircon grains were dated per sample, when possible, to obtain realistic and reliable detrital ZFT age populations (Table 1). Detrital grain-age populations were determined using statistical techniques (Brandon, 1996) (Table 1) and plotted against the stratigraphic age (Fig. 7) similar to that in Fig. 2. The stratigraphic ages (t_d) were based on previous studies of the AAB (Tschopp, 1953; Faucher & Savoyat, 1973; Bristow & Hoffstetter, 1977; Baldock, 1982; Balkwill *et al.*, 1995; Barragan *et al.*, 1997; Jaillard, 1997; Christophoul, 1999; Zambrano *et al.*, 1999; Christophoul *et al.*, 2002a) but also by dating of syn-depositional volcanic contamination (see below).

Heavy-mineral suites of all the samples taken for thermochronological analysis were also studied in order to: (1) assess variation of source materials with any changes in detrital thermochronology and (2) identify any major input of volcanic material which would yield zero lagtime and may have an influence on the pattern of the thermochronological data sets. The preparation followed standard procedures (Mange & Maurer, 1992). Sandstones were crushed and the 2–4-mm fraction was dissolved in 10% acidic acid to remove carbonate cement. Bromoform ($\rho = 2.88$) density separation was carried out on the sieve fraction 0.063–0.4 mm. The heavy-mineral fraction was mounted in piperin and at least 200 grains were counted using a petrographic microscope.

Results

Many rounded and zoned pink zircons, mainly from the oldest sedimentary formations, were undatable because they were either too damaged or the spontaneous track density was too high to count. Although this leads to bias in the data set, it was not important in this study because the main focus is the analysis of the younger populations that trace the younger hinterland development. Most results had mean ages with a $P(\chi^2)$ value (Green, 1981) lower than 5%, thus supporting the presence of multiple populations (Table 1). Most of the dated samples yield several populations ($1 < n < 5$, Table 1). In general at each site two or more populations could be distinguished. Three D_n-type curves are readily apparent – D_1, D_2 and D_3 curves based on the lines joining the various populations. These lines are remarkably similar particularly in the change of the lagtime up-section. Seven sites yielded age-populations statistically identical to the stratigraphic age (Fig. 7) and are discussed below.

The variable heavy mineral compositions of the sandstones of the SAZ are summarised in Fig. 8. The lower half of the section dominantly contains minerals associated with granitoid sources, e.g. zircon, tourmaline, rutile (ZTR association) but by the Santonian, metamorphic

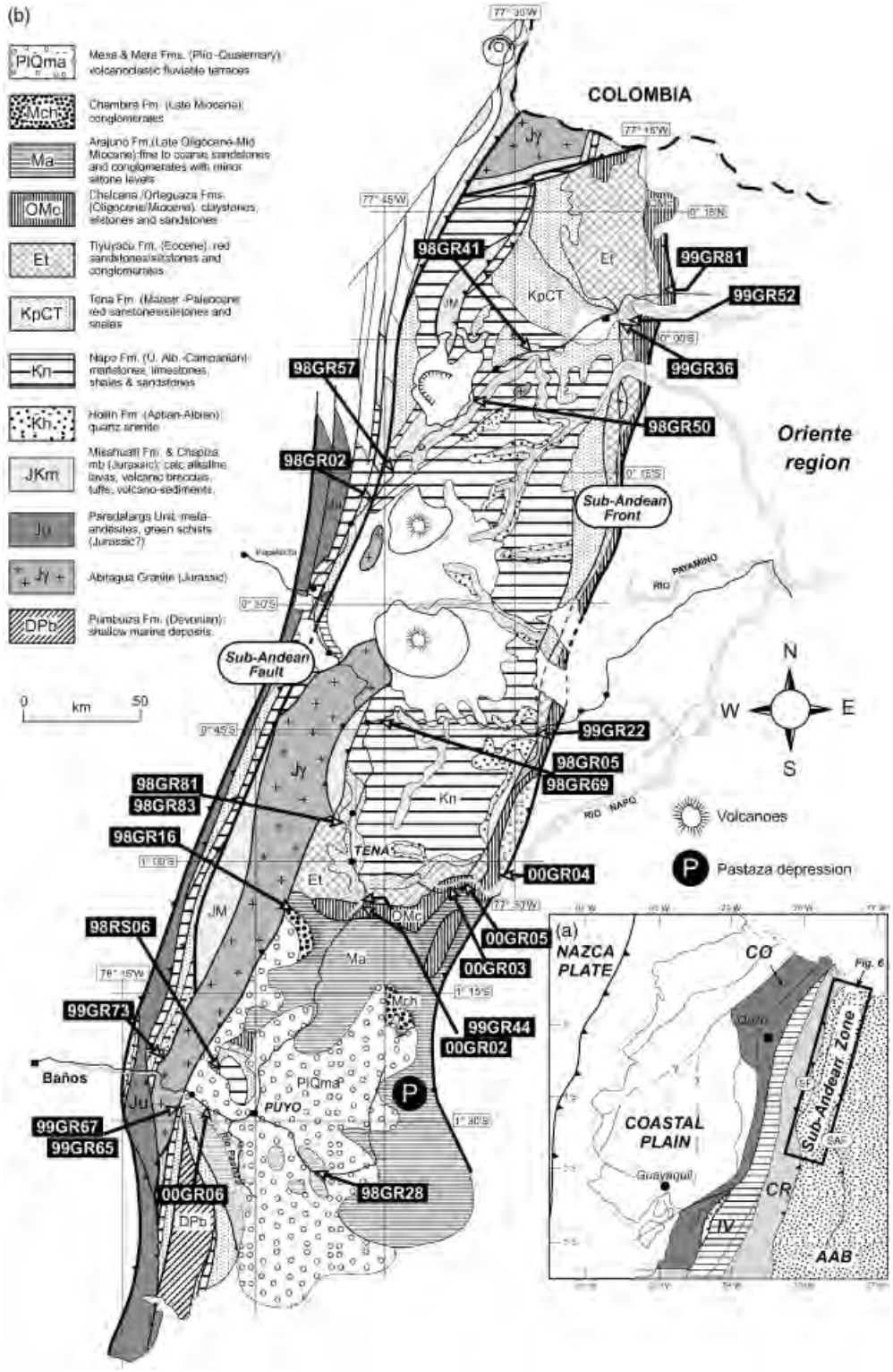

Fig. 6. (a) Morpho-tectonic sketch of the Ecuadorian Andes (adapted from Guillier *et al*., 2001). CO, IV, CR, SF, SAF: Western Cordillera, Interandean Valley, Cordillera Real, Sub-Andean Fault, Sub-Andean Front. Highlighted and detailed in (b) is the geological map of studied area, i.e. the northern Ecuadorian Sub-Andean Zone referred to as the Napo region and Pastaza depression (modified after Litherland *et al*., 1993), with sample locations.

minerals were being introduced and increase upwards with time. From the Upper Eocene to Upper Miocene, high-grade metamorphic minerals such as kyanite and sillimanite increase in abundance. From the Upper Miocene, the input was dominantly augite, olivine and hypersthene derived from mafic volcanic source rocks. A modern river sand, from the Napo River, yielded a complex mixture of the three different groupings listed above.

Table 1. Detrital zircon fission-track (ZFT) ages from the Aptian to recent sediments of the northern Ecuadorian Sub-Andean Zone.

Sample Number	UTM	UTM	N	$P\chi^2$ %	C. Age ± 1σ (Ma)	P_1 ± 1σ (Ma)	P_2 ± 1σ (Ma)	P_3 ± 1σ (Ma)	P_4 ± 1σ (Ma)	P_5 ± 1σ (Ma)	St. (Ma)	L_{gl} (Myr) ± 1σ
00GR05 (Qt)	–	–	37	0.0	59 ± 5	30 ± 5 (4)	50 ± 3 (23)	142 ± 13 (10)	–	–	0	30 ± 5
00GR06 (Ms)	184 083	9 820 200	25	0.0	49 ± 7	43 ± 2 (16)	57 ± 6 (8)	255 ± 84 (1)	–	–	4	39 ± 2
98GR16 (Ch)*	176 850	9 883 480	46	0.0	61 ± 3	45 ± 4 (14)	60 ± 7 (18)	80 ± 7 (13)	242 ± 49 (1)	–	9	36 ± 4
Arajuno Fm. (Early to Middle Miocene)												
98GR28*	183 856	9 82 555	40	0.0	63 ± 4	56 ± 3 (38)	198 ± 33 (2)	–	–	–	16	40 ± 3
00GR04	216 517	9 882 580	55	0.0	57 ± 5	23 ± 1 (6)	49 ± 3 (26)	70 ± 5 (10)	115 ± 9 (8)	330 ± 48 (5)	22	0 ± 1
00GR04 (ap.)	*216 517*	*9 882 580*	*27*	*68.8*	*19.3 ± 1.5*	*19.3 ± 1.5*	–	–	–	–	*22*	*0 ± 1.5*
Chalcana Fm. (Late Oligocene–Early Miocene)												
00GR03	212 561	9 886 172	56	0.3	55 ± 5	50 ± 3 (38)	70 ± 6 (18)	–	–	–	24	26 ± 3
00GR02	189 475	9 879 828	29	17.0	60 ± 3	60 ± 3 (29)	–	–	–	–	27	33 ± 3
Orteguaza Fm. (Late Eocene–Oligocene)												
99GR81*	246 500	N9350	23	0.0	98 ± 7	77 ± 5 (12)	123 ± 8 (11)	–	–	–	32	45 ± 5
Tiyuyacu Fm. (Eocene)												
99GR44	189 343	9 880 298	51	0.0	56 ± 5	36 ± 4 (4)	53 ± 3 (30)	70 ± 5 (17)	–		36	0 ± 4
98GR81	185 967	9 896 510	25	0.0	69 ± 5	67 ± 3 (24)	269 ± 46 (1)	–	–	–	44	23 ± 3
99GR52*	242 139	N4314	10	57.0	234 ± 31	234 ± 31 (10)	–	–	–	–	50	184 ± 31
99GR36	244 995	N3650	24	0.0	57 ± 7	51 ± 5 (4)	73 ± 6 (8)		–	–	51	0 ± 5
Tena Fm. (Maastrichtian–Early Palaeocene)												
98GR83	185 967	9 896 510	35	13.7	65 ± 07	63 ± 3 (34)	242 ± 72 (1)	–	–	–	59	0 ± 3
99GR67	150 510	9 936 429	30	0.0	106 ± 13	72 ± 3 (20)	232 ± 40 (1)	494 ± 44 (9)	–	–	70	2 ± 3
Napo Fm. (Middle–Early Cretaceous)												
98RS06	160 050	9 842 950	54	0.0	189 ± 20	86 ± 6 (16)	224 ± 20 (18)	481 ± 35 (20)	–	–	86	0 ± 6
98GR41*	224 435	9 998 965	49	0.4	247 ± 18	153 ± 13 (16)	335 ± 23 (33)	–	–	–	90	63 ± 13

Table 1. (Continued)

Sample Number	UTM	UTM	N	$P\chi^2$ %	C. Age ± 1σ (Ma)	P_1 ± 1σ (Ma)	P_2 ± 1σ (Ma)	P_3 ± 1σ (Ma)	P_4 ± 1σ (Ma)	P_5 ± 1σ (Ma)	St. (Ma)	L_{g1} (Myr) ± 1σ
98GR57*	196 101	9 973 320	16	2.1	188 ± 26	139 ± 18 (9)	323 ± 69 (7)	–	–	–	99	40 ± 18
98GR02	191 210	9 968 100	57	0.0	263 ± 24	101 ± 11 (6)	267 ± 22 (36)	516 ± 43 (15)	–	–	101	0 ± 11
Hollin Fm. (Alb.–Apt.)												
99GR73*	144 450	9 844 850	29	0.0	227 ± 30	118 ± 11 (10)	301 ± 45 (10)	579 ± 65 (9)	–	–	105	13 ± 11
99GR22*	223 150	9 918 125	50	0.0	284 ± 22	150 ± 6 (10)	355 ± 23 (40)	–	–	–	107	43 ± 16
98GR69*	193 292	9 919 767	45	0.0	298 ± 29	134 ± 16 (7)	227 ± 33 (11)	518 ± 32 (27)	–	–	110	24 ± 16
98GR50*	212 376	9 989 981	33	0.0	258 ± 25	174 ± 11 (15)	359 ± 48 (11)	569 ± 85 (7)	–	–	112	62 ± 11
98GR05*	187 585	9 921 730	61	0.0	285 ± 26	139 ± 8 (16)	426 ± 24 (45)	–	–	–	113	26 ± 8
99GR65*	149 450	9 936 250	31	0.0	316 ± 40	128 ± 10 (6)	309 ± 44 (6)	506 ± 45 (19)	–	–	115	13 ± 10

The different age-populations have been separated using statistical techniques (Brandon, 1996) and labelled as P_1 to P_5 with increasing ages. The stratigraphic age (St.) of each dated level is indicated as the lagtime associated with the P_1 population (L_{g_1}) in Myr. Italic corresponds to an Arajuno sample (00GR04) that yielded an AFT age identical to its youngest P_1 ZFT population. Asterisks correspond to samples with poorly constrained stratigraphic ages ($1\sigma \sim > 3$ Myr, Ruiz, 2002). Numbers in parentheses indicate the number of grains per population while N is the number of dated grains per sample. Alb.–Apt.: Albian–Aptian; C. Age: central age; Ch, Chambira; Ms, Mesa; Qt, Quaternary. Zircon and apatite separates were counted by G.M.H. Ruiz using a ξ calibration factors of 121 ± 3 (oil, CN1 standard glass, ×1600 magnification) and 359 ± 11 (CN5 standard glass, ×1250 magnification), respectively, and irradiated at the ANSTO facility, Lucas Heights, Australia.

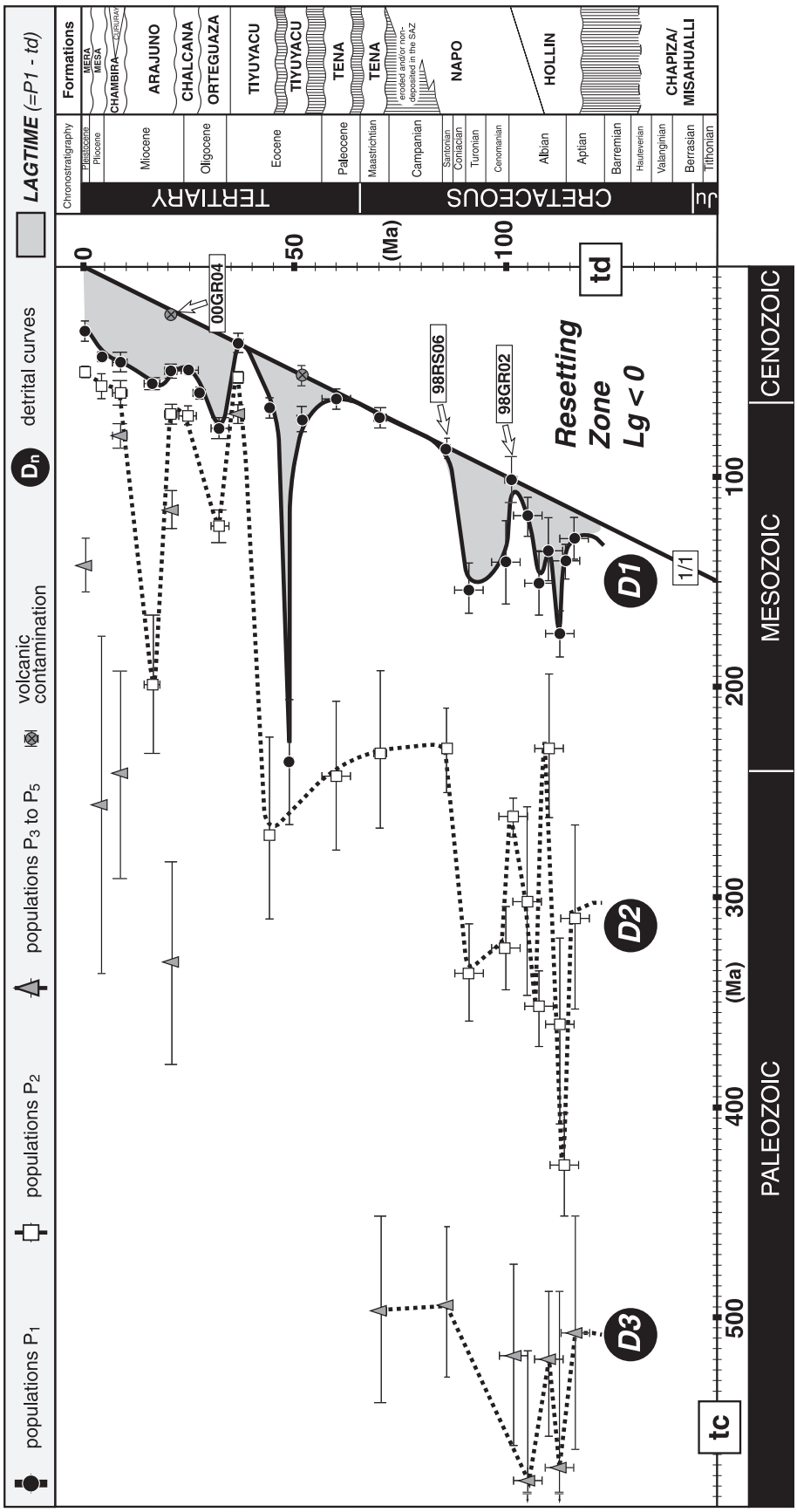

Fig. 7. Detrital zircon fission-track data set from northern Ecuador. The *y*-axis represents the stratigraphic age (t_d) of the hosting sediment and the *x*-axis is the thermochronological age of the detrital population (t_c). Within the data set some levels yielded up to five populations but because all did not, only three detrital curves D_1, D_2 and D_3 linking the P_1, P_2 and P_3 populations are drawn where possible. The area between the 1 : 1 correlation line and the D_1 curve (dark grey) represents the evolution of the lagtime omitting the contemporaneous volcanic populations, which were discriminated using a combination of mineral associations especially heavy minerals. Error bars are $\pm$ 1 standard deviation for population ages.

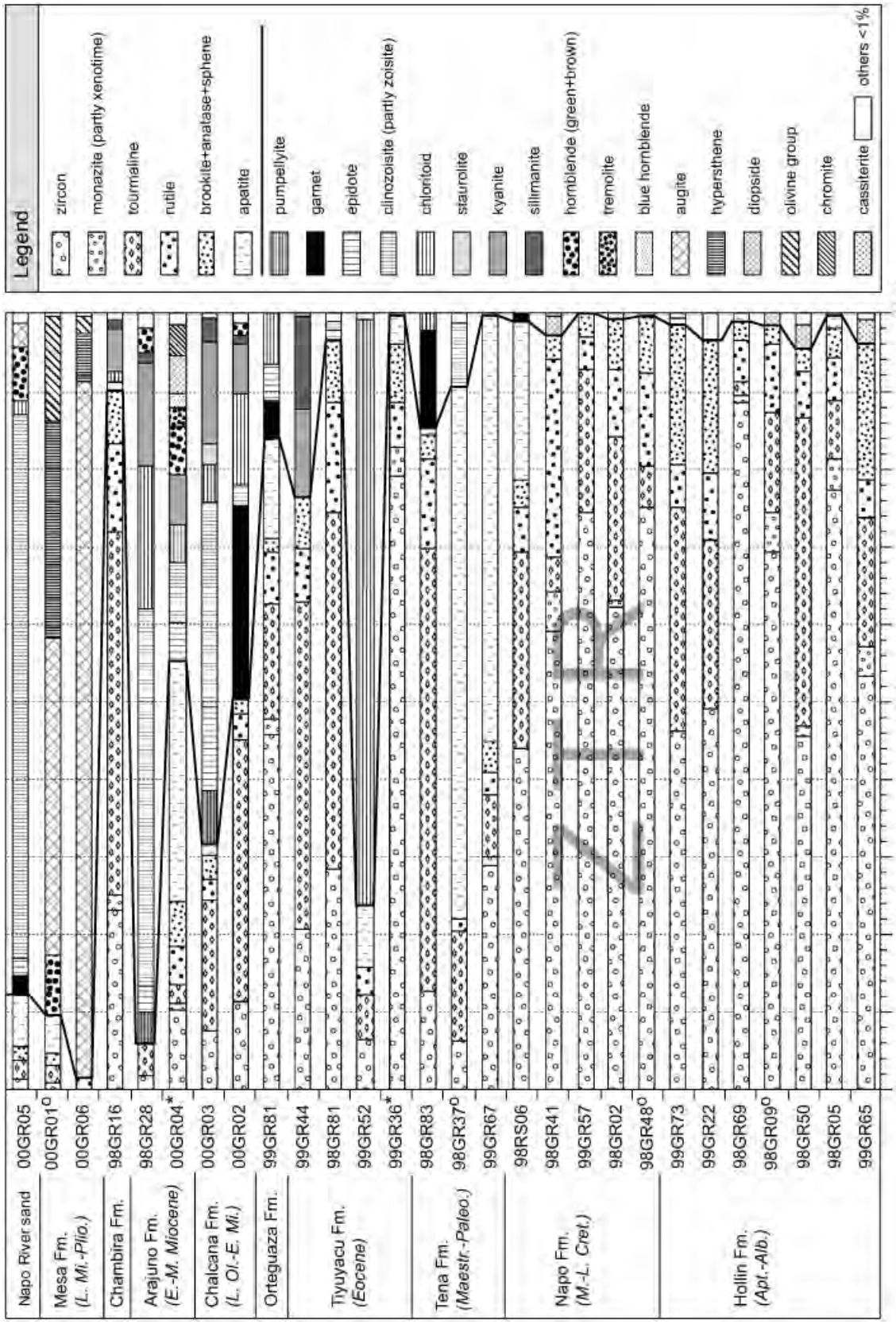

Fig. 8. Heavy-mineral occurrences (frequency present) in the Aptian to Recent basin fill series from the Ecuadorian AAB in the northern SAZ. Stratigraphic order from base to the top. Samples marked with open circle: no detrital fission-track ages available. Samples marked with asterix: a contemporaneous volcanic contamination to the detrital material is evident. The bold line separates the zircon–tourmaline–rutile association (ZTR) and apatite from other heavy minerals to highlight the trends in grain associations. The density separation was carried out on the 0.063–0.4 mm fraction in bromoform (density 2.88). The grains were mounted in piperin (refractive index 2.67). More than 200 grains were counted in each mount.

Interpretation

Zero lagtime

Seven sites yield ages statistically identical to the stratigraphic age. With the combination of heavy-mineral analysis, it was possible to discern which of these represented contemporaneous volcanic input (volcanic fragments, euhedral elongate zircons, euhedral mafic minerals such as hornblende and biotite). Two such cases were uncovered, and were therefore not incorporated into the D_1 curves (Fig. 7). However, they were useful ages in the sense that they radiometrically date the age of the hosting sediment (Table 1). The other zero lagtime ages must be interpreted as indicative of rapid exhumation because no evidence of syn-sedimentary volcanic contamination was present.

Aptian–Turonian

The Hollin and Napo fms. contain three distinct populations. P_2 and P_3, (Fig. 7) had relatively old zircons (>220 Ma) compared with the stratigraphic ages of the dated strata (110–90 Ma) and are commonly associated with the resistant minerals of the ZTR pole (Fig. 8), i.e. zircon, tourmaline and rutile (Mange & Maurer, 1992). The P_3 zircons are characteristically dark and rounded. They may have passed through more than one sedimentary cycle but their earlier host rocks may have been the shield regions and its Palaeozoic platform cover (Tschopp, 1953; Bristow & Hoffstetter, 1977; Baldock, 1982; Rivadeneira & Baby, 1999) located to the east of the SAZ (Fig. 6). The source terranes of the P_2 populations with Palaeozoic ZFT ages (Table 1) could be either the Palaeozoic cover sequences of the eastern shield region or the exhuming proto-Cordillera Real (Fig. 6). The P_1 populations, present in the early deposits of the AAB, range between 174 and 101 Ma (Table 1). This is a similar time span to that identified by Ruiz (2002) using ZFT analysis on the Jurassic volcanics of the Misahualli Fm. that partly constitute the basement of the northern SAZ. Much of this basement is now missing in the central part of the SAZ as evidenced by a 50 Myr hiatus between the Misahualli and Hollin Fms. (Ruiz, 2002) but also further east, in the AAB (Tschopp, 1953; White *et al.*, 1995). Hence, it may be that these P_1 populations represent some of this eroded material. The peneplenation of the entire AAB at a time between 140 and 110 Ma had already been noted by Tschopp in 1953. This phase probably postdated the accretion of allochtonous terranes against the northern Andean segment, referred as the Peltetec event (Litherland *et al.*, 1994), which was a consequence of the rearrangement of the subduction regime in the Pacific realm between 140 and 100 Ma (Duncan & Hargraves, 1984) and responsible for the cessation of the Misahualli arc. Although the heavy-mineral suites of the Hollin and Napo Fms. are not typical of the volcanics, this does not eliminate the possibility of the volcanic pile as a source because plagioclase and devitrified glass dominate the modal composition of the Misahualli pile (Wasson & Sinclair, 1927; Romeuf *et al.*, 1995). Further, any eroding material from this pile, including zircons, may have passed into the poorly studied red beds of Jurassic to Early Cretaceous age, otherwise referred to as the Chapiza Fm. (Tschopp, 1953), eliminating then the unstable volcanic phases. The low precision of the stratigraphic ages of the quartz arenites from the Hollin and Napo Fms. (Fig. 7, Table 1) unfortunately precludes the construction of reliable paths along the D_n ZFT curves for the Aptian to Cenomanian. Consequently, the lagtime of the P_1 populations cannot be utilised to determine reliable estimates of the contemporaneous exhumation rate in the hinterland. In addition, several Cretaceous igneous bodies (106–84 Ma, Barragan *et al.*, 1997) are reported intercalated within the Napo Fm. in both the AAB and SAZ (Ruiz, 2002); they are located above structures re-activated during a transpressional regime (Rivadeneira & Baby, 1999). Such bodies may have contributed detritus to sample 98GR02 during an eastward transgressive episode, resulting in its young P_1 population of 101 ± 11 Ma (Table 1) even if no volcanic signature was evidenced from its heavy-mineral assemblage. However, the large error (± 11 Ma) leaves the question as to the reality of the zero lagtime.

Coniacian–Palaeocene

Two to three populations are again identified in this time span (Table 1). At the base, clear type 5 paths with characteristic decreasing lagtime values are evident along both the D_1 and D_2 curves for the upper Cretaceous using the well-constrained Santonian stratigraphic age (Jaillard, 1997) of an upper Napo sample (98RS06, Table 1). This change to faster exhumation with a minimum rate of $1\,\mathrm{mm\,yr^{-1}}$ using a maximum lagtime value of 6 Myr (Garver *et al.*, 1999) for the D_1 curve (Fig. 7) is associated with the first appearance of low- to medium-grade metamorphic minerals in the heavy-mineral detritus of the Upper Napo Fm. (Fig. 8). Because such high exhumation rates are rarely documented in cratonic regions (Harman *et al.*, 1998), such as those located to the east of the SAZ (Fig. 6), one can conclude that the Coniacian to Santonian more likely represents a period of exhumation in the proto-Ecuadorian Andes to the west of the AAB. This can be correlated with the reported synchronous basin inversion in the AAB (Rivadeneira & Baby, 1999) and reported compressive episode in the Colombia Andes further north (Dengo *et al.*, 1993; Cooper *et al.*, 1995). Such an orogenic phase was probably related to the docking of an oceanic plateau complex (Cosma *et al.*, 1998; Lapierre *et al.*, 2000), referred to as the Pallatanga Terrane (Fig. 6) along the western forearc of Ecuador (Hughes & Pilatasig, 2002). In addition, the heavy-mineral assemblages become progressively more heterogeneous and the proportion of medium-grade metamorphic mineral grains increases stratigraphically upwards from the Maastrichtian-Palaeocene Tena Fm. (Fig. 8). Simultaneously, the detrital ZFT record becomes less disperse from the Tena Fm. with the proportion of older ZFT populations almost disappearing (Fig. 7). If the oldest group of ZFT ages is assumed to have

been primarily derived from shield regions and their sedimentary cover to the east of the SAZ (Fig. 6), their absence in the Palaeocene series suggests that the supply from this region was most likely lacking (Fig. 7). From Santonian time, the D_1 curve is characterised by a type 4 path with an approximately zero lagtime that persists to a time somewhere between the deposition of the upper Tena and basal Tiyuyacu deposits of Early Eocene age (Faucher & Savoyat, 1973; Bristow & Hoffstetter, 1977; Fig. 7) implying exhumation greater than 1 mm yr^{-1} for this period in the hinterland (Table 1). However, such a rate would also imply that 35 km of material was eroded if such a rate was sustained over this time period. Such a long period of rapid exhumation is probably unlikely. At least two periods of erosion or non-deposition have been identified in this time span (Fig. 7) – it is thus possible that similar fluctuations also occurred in the source rocks. Further, these sediments contain garnet and chloritoid. Higher temperature phases do not come into the basin until the upper Eocene (Fig. 8). The drop in contribution of detritus from the east revealed by both the loss of the older population, and the heavy mineral suites indicates that the shield regions to the east had been progressively buried beneath the basin fill sequence of the AAB since at least the Maastrichtian, whereas rapid exhumation occurred to the west of the AAB. This orogenic development of the Ecuadorian Andes is supported by fission-track and $^{40}Ar/^{39}Ar$ analyses from the Cordillera Real located to the east of the AAB (Fig. 5; Spikings *et al.*, 2000, 2001). It is corroborated (i) by a switch in current direction from an eastern to a western source for the Tena Fm., suggesting that the input and hence the erosion of the eastern margins may have decreased (e.g. Tschopp, 1953; Balkwill *et al.*, 1995); (ii) with a major change in the depositional environment, in that the Napo Fm. was shallow marine and the Tena Fm. clearly continental, with continental red beds, shales, sandstones, siltstones and some conglomerates (Jaillard, 1997) but also (iii) an increase in tectonic subsidence (Jaillard, 1997) indicating the presence of an orogenic load to the west of the basin.

Eocene

The oldest Eocene sample, from the Tiyuyacu Formation, is a conglomerate which contains one population with a zero lagtime (Table 1) (Fig. 7). The presence of tuffaceous cement, phosphatic matter and idiomorphic zircons probably support sourcing from a volcanic series. These idiomorphic zircons yielded a ZFT population with an age of 51 ± 5 Ma (Table 1). Consequently, the P_1 population was excluded from the D_1 curve but it allowed the stratigraphic age of the horizon to be constrained. This population is replaced by the second youngest population of 73 ± 6-Ma age (Table 1), initiating a type 1 path along the D_1 curve (Fig. 7). This is coupled with the disappearance of metamorphic minerals and the exclusive presence of a ZTR assemblage (Fig. 8) to suggest a clear change of source region by Late Palaeocene–Early Eocene. The pebbles of this level are dominantly composed of 10–12-cm, sub-rounded, radiolarian black chert (Ruiz, 2002). Thus, the drainage system of the AAB was clearly modified by the Early Eocene such that source rocks changed towards pelagic sediments of an oceanic domain, contemporaneous volcanic centre(s), but also shallow continental crustal levels (ZTR; Mange & Maurer, 1992). Interestingly, this P_2 ZFT population of 73 ± 6 Ma (± 1σ), is indistinguishable from the P_1 populations from the underlying Tena Fm., i.e. 72 ± 3 and 63 ± 3 Ma (Fig. 7; Table 1) and a major erosive unconformity exists between both formations (Tschopp, 1953; Rivadeneira & Baby, 1999). It is thus likely that the Tena Fm. was partly reworked into the basal strata of the Tiyuyacu Fm. Another possible source for these deposits, which also sourced the Tena Fm., was that the Pallatanga Terrane today located in the Cordillera Occidental (Hughes & Pilatasig, 2002; Fig. 6). The Yunguilla Fm. of Maastrichtian–Palaeocene age (71–65 Ma) composes part of this terrane and is characterised by both its syn-accretionary signature (Hughes & Pilatasig, 2002) but also the presence of radiolarian cherts characteristic of the base of the Yunguilla Formation (Jaillard *et al.*, 2002a). Notably, the presence of pelagic radiolarian chert clasts in the Lower Tiyuyacu Mb. (Early Eocene) indicates that sedimentary series associated with the Pallatanga Terrane may have contributed to the flux of clastic material. Furthermore, Pecora *et al.* (1999) suggested that in the Late Palaeocene a buoyant basaltic plateau, referred to as the Piñon block (Fig. 5; Jaillard *et al.*, 1997), accreted against the northernmost margin of Peru. It later migrated north-eastward along dextral wrench faults to its present day location where it defines the basement of the coastal region (Jaillard *et al.*, 1997, Fig. 6). According to Kerr et *al.* (2002), this phase was synchronous with the accretion of oceanic terranes to the north of the Ecuadorian margin. Early Eocene thrusting and exhumation related to the accretion of these terranes are in complete agreement with reported synchronous cooling ages from the southern part of the Cordillera Real (Spikings *et al.*, 2001).

A major type 5 path characterises the change in lagtime from 184 Myr to approximately zero over the Middle to Late Eocene (Fig. 7). This is recorded in both the D_1 and D_2 paths. Thus during the Middle-to-Late Eocene, rates of exhumation in the source region were probably > 1 mm yr^{-1} because of the ∼zero lagtime (Table 1). The presence of the two sub-parallel D_1 and D_2 curves suggests that two different hinterland blocks, were being rapidly denuded at this time. The abundance of high-grade detrital minerals, i.e. kyanite and sillimanite (Fig. 8) suggests erosion into deeper levels exposing high-grade metamorphic sequences that occur over a vast area in the present day Cordillera Real to the west (Litherland *et al.*, 1994).

In summary, and with regard to the evolution of the source terranes during deposition of the Tiyuyacu Fm., two events are recognized: (1) the Lower Tiyuyacu Mb. is characterised by a change of source terrane and (2) the Upper Tiyuyacu Mb. records exhumation of high-grade

metamorphic terranes during the Middle- and Late Eocene (44–36 Ma). The first may be interpreted as representing a radical tectonic rearrangement of the hinterland because of the accretion of the Piñon block, whereas the latter indicates a substantial exhumation that reached rates $> 1\,\mathrm{mm\,yr^{-1}}$. Moreover, this Middle-to-Late Eocene rapid exhumation period correlates with the 43–30 Ma peak of exhumation of the Cordillera Real (Spikings *et al.*, 2000, 2001). This orogenic phase is probably related to the Middle-to-Late Eocene docking of the Macuchi island arc against the Ecuadorian margin (Egüez, 1986; Hughes & Pilatasig, 2002) and correlates with the Late Eocene–Early Oligocene 'Incaic' phase of deformation (Steinmann, 1929; Noble *et al.*, 1979; Mégard, 1987; Clark *et al.*, 1990; Sandeman *et al.*, 1995), which is defined as a major phase of shortening in the Central Andes.

Early Miocene – Recent

A record of volcanic activity is evidenced in the Early Miocene. Pseudo-hexagonal biotites, hornblende, diopside, euhedral, inclusion-rich apatites and idiomorphic zircons in the basal Arajuno strata, combined with indistinguishable ZFT and AFT ages of 22 Ma ages (00GR04; Table 1) suggest that there was a contemporaneous volcanic supply (Fig. 7). Because of this volcanic contamination, the D_1 and D_2 paths spanning the upper Chalcana and Arajuno Fms. depict two type 2 paths (Fig. 7). These identical ZFT populations in both levels are associated to the (1) presence of identical mineral assemblages in both formations (Fig. 8) (with the exception of the chromite and volcanic detritus in the Arajuno Fm.) and (2) the unconformable contact between the Chalcana and Arajuno Fms. (Christophoul *et al.*, 2002a) to suggest the cannibalisation of the Chalcana Fm. into the Arajuno Fm.

The pattern of the detrital ages for the Middle Miocene to Recent follows simple type 4 paths for both D_1 and D_2 with constant lagtime values of $\sim$30–40 and 50 Myr, respectively (Fig. 7; Table 1). The constancy of these long lagtimes suggests averaged low exhumation rates in the source regions of these deposits from the Middle Miocene, but most likely from the Late Palaeocene–Early Eocene, if we consider the age of the first population along this type path for the D_1 curve, i.e. 56 ± 3 Ma (Table 1) (Fig. 7), to Recent. It is also very tempting to conclude that these source regions of the AAB were until today in a thermal steady state (Willett & Brandon, 2002). However, AFT ages associated with ZFT and $^{40}Ar/^{39}Ar$ ages from the Cordillera Real (Spikings *et al.*, 2000, 2001; Figs 5 and 6) clearly document different pulses of exhumation during the Tertiary. In addition (1) the complexities of the potential source regions (Litherland *et al.*, 1994), as well as (2) the very varied heavy-mineral detritus (Fig. 8), and also (3) the active fault systems observed today in the hinterland of the AAB (Litherland *et al.*, 1994; Guillier *et al.*, 2001) lead one to suspect that steady state cannot be a reality in the Ecuadorian Andes. Such long and constant lagtimes are thus probably the results of two deferred phases of exhumation that affected the same region(s) of the hinterland of the AAB at the same low rate, i.e. ~ 0.3–$0.4\,\mathrm{mm\,yr^{-1}}$ using 30–40-Myr values (Garver *et al.*, 1999): the second one exhuming to the surface the rocks the previous one cooled through the temperature of closure for ZFT.

Using FT analysis, Spikings *et al.* (2001) evidenced that both the western Cordillera and Inter-Andean region were probably affected by a phase of exhumation since 5 Ma. Such phase is not seen yet through changes in the detrital ZFT patterns from the northern Ecuadorian SAZ deposits (Fig. 7) but rather through the clear appearance of mafic detritus (Fig. 8) that was most likey derived from these exhuming regions constituted of accreted oceanic terranes (Fig. 5).

CONCLUSIONS

We have presented a method allowing the recognition of tectonic events in the source regions of sedimentary basins, recorded through the ages of detrital grains from the enclosing sediments. This has been tested in a combined heavy-mineral study in the northern Ecuadorian SAZ.

Five different paths have been identified which may be interpreted in the light of tectonic activity in the source region. The principal factor governing the different paths is the temporal change in lagtime. The application can be used with any suitable datable mineral phase. In order to confirm that the dated grains yield a true detrital signature, the application of AFT analysis is ideal.

The dated grains for each horizon are separated into populations ($P_1 - P_n$) and plotted at their stratigraphic level. The corresponding P_n populations are joined through time yielding the D_n curves. Identification of volcanic contamination characterised by zero lagtime value, is made via the heavy-mineral suites. The safest D_n curve to interpret is the youngest, or D_1, because older paths are more likely to contain recycled material and must be assessed with caution. Even so, in the example we present, the parallelism of the different D_n curves is strong and suggests that the correct junctions have been made between the different P_n points.

An example using ZFT analysis from the SAZ, eastern Ecuador, illustrates well that different paths can be correlated with known events in the probable source regions as summarised below:

(a) There is a general younging trend upwards in the column. This is expected as sources are continually being exhumed with time.
(b) The oldest curve (D_3) remained in the sequence from Aptian until the end of the Cretaceous when it very abruptly disappeared. It contains ages that are in general > 500 Ma with a long lagtime, indicative of very slow cooling or possible reworking. The source region was most likely the Guyana Shield to the east. This abrupt disappearance at the end of Cretaceous times is associated with changes in palaeocurrent direction, lithology and facies in the AAB and synchronous with the onset of a period of rapid exhumation in the

Cordillera Real recorded through the detrital zircon ages. This is the time when the main detrital supply switched from the shield region in the east, to the Cordilleras in the west. This phase is clearly coincident with the docking of the oceanic Pallatanga Terrane at ~90 Ma against the Ecuadorian margin which must have caused rapid exhumation to the west of the basin. At its peak approximately zero lagtimes were recorded pointing to high exhumation rates ($>1\,mm\,yr^{-1}$). At about 85 Ma is the first signature of metamorphic minerals into the basin with a general increase until about ~55 Ma. This increase is associated with a proportional decrease of the mineral phases associated with the shield regions. The rising Cordilleras were being more deeply eroded.

(c) At about 55 Ma there was a sudden reversion to a shallow continental ZTR signature. At the same time, volcanic material was introduced into the basin. It is correlated with a remarkable pulse to a type 1 path and is interpreted as a change in source region. From about 48–37 Ma, a strong type 5 path has been dominating and the incoming of sillimanite and kyanite suggests a continued phase of rapid erosion, cutting deeper into the source region. This highly variable path in the Eocene implies strong tectonic impacts at this time with related switching of sources because of the collision of the Piñon and Macuchi terranes on the western margin.

(d) From ~37 Ma, the lagtime associated to the P_1 populations increased to about 30–40 Myr and has remained somewhat constant around this figure since then. A metamorphic mineral source most likely from the Cordillera Real dominates until about 5 Ma when there was a strong input of minerals associated with basic volcanic material derived from the uplifting Cordillera Occidental and Inter-Andean region.

(e) The modern-day Napo River sand is characterised by a dominance of clinozoisite but also has a combination of the late volcanic material as well as a small proportion of granitic source minerals. This river drains from the western Cordillera Occidental across the metamorphic Cordillera Real cutting the large granite batholiths such as the Abitagua. It also has the approximate 30 Myr lagtime associated with the sequences as far back as ~30 Ma. The detrital grain ages taken alone suggest that the source regions of the SAZ were in thermal steady state for approximately the last 30 Myr. However, there is abundant other evidence that the region is variously active. AFT data (Spikings *et al.*, 2001; Ruiz, 2002) have shown the variability with very young ages close to some of the large faults associated with Pliocene movement. Steady state is thus a matter of scale.

ACKNOWLEDGEMENTS

We wish to thank three reviewers for the their comments in improving this manuscript, John Garver, Cornellia Spiegel and Patrice Baby. Special thanks also go to Richard Spikings and Alexandre Kounov for their enthusiasm and discussion in the laboratory. The research was supported by grant number SNF no. 21-050844.97

REFERENCES

Baldock, J.W. (1982) Geología del Ecuador. Boletín de Explicación del Mapa geológico de la Républica del Ecuador. Dirección General de Geología y Minas, Quito, p. 70.

Balkwill, H.R., Rodrigue, G., Paredes, F.I. & Almeida, J.P. (1995) Northern part of the Oriente basin, Ecuador: reflexion seismic expression of structures. *AAPG Mem.*, **62**, 559–571.

Barker, C. (1996) *Thermal Modeling of Petroleum Generation: Theory and Applications*. Elsevier, Amsterdam.

Barragan, R., Ramirez, F. & Rodas, J. (1997) Evidence of an Intra Plate 'Hot Spot' under the Ecuadorian Oriente Basin during the Cretaceous tectonic evolution. *VI Simposio Bolivariano 'Exploración Petrolera en las cuencas Subandinas'*, Cartagena de Indias, Colombia, pp. 99–104.

Bernet, M., Zattin, M., Garver, J.I., Brandon, M.T. & Vance, J.A. (2001) Steady-state exhumation of the European Alps. *Geology*, **29**, 35–38.

Blenkinsop, T.G. (1988) Definition of low-grade metamorphic zones using illite crystallinity. *J. Metamorph. Petrol.*, **6**, 623–636.

Brandon, M.T. (1996) Probability density plot for fission-track grain-age samples. *Radiat., Meas.*, **26**, 663–676.

Brandon, M.T. & Vance, J.A. (1992) Fission-track ages of detrital zircon grains: implications for the tectonic evolution of the Cenozoic Olympic subduction complex. *Am. J. Sci.*, **292**, 565–636.

Brandon, M.T., Roden-Tice, M.K. & Garver, J.I. (1998) Late Cenozoic exhumation of the Cascadia accretionary wedge in the Olympic Mountains, NW Washington State. *Geol. Soc. Am. Bull.*, **110**, 985–1009.

Brewer, I.D., Burbank, D.W. & Hodges, K.V. (2003) Modelling detrital cooling-age populations: insights from two Himalayan catchments. *Basin Res.*, **15**, 305–320.

Bristow, C.R. & Hoffstetter, R. (1977) Ecuador. In: *Lexique Stratigraphique International*, **Vol. 5a2.** *2ème édn.*, CNRS, Paris.

Brügel, A., Dunkl, I., Frisch, W., Kuhlemann, J. & Balogh, K. (2003) Geochemistry and geochronology of gneiss pebbles from foreland molasse conglomerates: geodynamic and paleogeographic implications for the Oligo-Miocene evolution of the Eastern Alps. *J. Geol.*, **111**, 543–563.

Burnham, A.K. & Sweeney, J.J. (1989) A chemical kinetic model of vitrinite reflectance maturation. *Geochim. Cosmochim. Acta*, **53**, 2649–2657.

Carrapa, B., Wijbrans, J. & Bertotti, G. (2003) Episodic exhumation in the Western Alps. *Geology*, **31**(7), 601–604.

Carter, A. (1999) Present status and future avenues of source region discrimination and characterization using fission track analysis. *Sediment. Geol.*, **124**, 31–45.

Carter, A. & Bristow, C.S. (2003) Linking hinterland evolution and continental basin sedimentation by using detrital zircon thermochronology: a study of the Khorat Plateau Basin, eastern Thailand. *Basin Res.*, **15**, 271–285.

Carter, A. & Moss, S.J. (1999) Combined detrital–zircon fission-track and U-Pb dating: a new approach to understanding hinterland evolution. *Geology*, **27**, 235–238.

Cerveny, P.F., Naeser, N.D., Zeitler, P.K., Naeser, C.W. & Johnson, N.M. (1988) History of uplift and relief of the Himalaya during the past 18 million years: evidence from

fission-track ages of detrital zircons from sandstones from the Siwalik Group. In: *New Perspectives in Basin Analysis* (Ed. by K.L. Kleinspehn & C. Paola), pp. 43–61. Springer-Verlag, New York.

Christophoul, F. (1999) Discrimination des influences tectoniques et eustatiques dans les bassins liés à des zones de convergence: exemples du bassin Subandin d'Équateur. PhD Thesis, University of Toulouse III.

Christophoul, F., Baby, P. & Dávila, C. (2002a) Stratigraphic response to a major tectonic event in a foreland basin: the Ecuadorian Oriente basin from Eocene to Oligocene times. *Tectonophysics*, **345**, 281–298.

Christophoul, F., Baby, P., Soula, J.C., Rosero, M. & Burgos, J. (2002b) Les ensembles fluviatiles neogenes du bassin subandin d'Equateur et implications dynamiques. *C. R. Geosci.*, **334**, 1029–1037.

Clark, A.H., Farrar, E., Kontak, D.J., Langridge, R.J., Arenas, F., France, L.J., McBride, S.L., Woodman, P.L., Wasteneys, H.A., Sandeman, H.A. & Archibald, D.A. (1990) Geologic and geochronologic constraints on the metallogenic evolution of the Andes of southeastern Peru. *Econ. Geol.*, **85**, 1520–1583.

Colony, R.J. & Sinclair, J.H. (1932) Igneous and metamorphic rocks of Eastern Ecuador. *Ann. N.Y. Acad. Sci.*, **34**, (August), 1–54.

Cooper, M.A., Addison, F.T., Alvarez, R., Coral, M., Graham, R.H., Hayward, A.B., Howe, S., Martinez, J., Naar, J., Penas, R., Pulham, A.J. & Taborda, A. (1995) Basin development and tectonic history of the Llanos basin, Eastern Cordillera, and Middle Magdalena valley, Colombia. *AAPG Bull.*, **79**(10), 1421–1443.

Cosma, L., Lapierre, H., Jaillard, E., Laubacher, G., Bosch, D., Desmet, A., Mamberti, M. & Gabriele, P. (1998) Pétrographie et géochimie des unités magmatiques de la Cordillere occidentale d'Equateur (0°30'S): implications tectoniques. *Bull. Soc. Géol. France*, **169**, 739–751.

Dengo, C.A. & Covery, M.C. (1993) Structure of the Eastern Cordillera of Colombia: implications for trap styles and regional tectonics. *AAPG Bull*, **77**(8), 1315–1337.

Duncan, R.A. & Hargraves, R.B. (1984) The Caribbean–South American plate boundary and regional tectonics. *Bull. Geol. Soc. Am.*, **162**, 81–94.

Dunkl, I., Frish, W., Kuhlemann, J. & Brügel, A. (1998) Pebble-population-dating: a new method for provenance analysis. *Terra Nostra*, **98**(1), 45.

Egüez, A. (1986) Evolution Cénozoique de la Cordillière Septentrionale d'Equateur: les minéralisations associées. Unpublished PhD Thesis, Université Pierre et Marie Curie, Paris.

England, P. & Molnar, P. (1990) Surface uplift, uplift of rocks, and exhumation of rocks. *Geology*, **19**, 1173–1177.

Faucher, B. & Savoyat, E. (1973) Esquisse géologique des Andes de l'Equateur. *Rev. Géographie Phys. Géol. Dyn. (2)*, **XV**(fasc. 1–2), 115–142.

Gallagher, K. (1995) Evolving temperature histories from apatite fision-track data. *Earth Planet. Sci. Lett.*, **136**, 421–435.

Garver, J.I. & Brandon, M.T. (1994) Erosional denudation of the British Columbia Coast Ranges as determined from fission-track ages of detrital zircon from the Tofino basin, Olympic Peninsula, Washington. *Geol. Soc. Am. Bull.*, **v. 106**, 1398–1412.

Garver, J.I., Brandon, M.T., Roden-Tice, M. & Kamp, P.J.J. (1999) Erosional denudation determined by fission-track ages of detrital apatite and zircon. In: *Normal Faulting, Ductile Flow, and Erosion* (Ed. by U. Ring, M.T. Brandon, S. Willett & G. Lister), *Exhumation Process: Geol. Soc. London Spec. Publ.*, **154**, 283–304.

Gleadow, A.J.W., Hurford, A.J. & Quaife, R.D. (1976) Fission-track dating of zircon: improved etching techniques. *Earth Planet. Sci. Lett.*, **33**, 273–276.

Green, P.F. (1981) A new look at statistics in fission-track dating. *Nucl. Tracks Radiat. Meas.*, **5**, 77–86.

Green, P.F., Duddy, I.R., Laslett, G.M., Hegarty, K.A., Gleadow, A.J.W. & Lovering, J.F. (1989) Thermal annealing of fission tracks in apatite – Qualitative modelling techniques and extensions to geological timescales. *Chem. Geol.*, **79**, 155–182.

Guillier, B., Chatelain, J.-L., Jaillard, É., Yepes, H., Poupinet, G. & Fels, J.-F. (2001) Seismological evidence on the geometry of the orogenic system in central-northern Ecuador (South America). *Geophys. Res. Lett.*, **28**(19), 3749–3752.

Harman, R., Gallagher, K., Brown, R., Raza, A. & Bizzi, L. (1998) Accelerated denudation and tectonic/geomorphic reactivation of the cratons of northeastern Brazil during the Late Cretaceous. *J. Geophy. Res., B, Solid Earth Planets*, **103**, 27091–27105.

Hughes, R.A. & Pilatasig, L.F. (2002) Cretaceous and Tertiary terrane accretion in the Cordillera Occidental of the Andes of Ecuador. *Tectonophysics*, **35**, 29–48.

Hurford, A.J. & Carter, A. (1991) The role of fission track dating in discrimination of provenance. In: *Developments in Sedimentary Provenance Studies* (Ed. by A.C. Morton, S.P. Todd & P.D.W. Haughton) Geol. Soc. Spe. Publi., **57**, 67–78.

Hurford, A.J. & Green, P.F. (1983) The zeta calibration of fission-track dating. *Chem. Geol.*, **1**, 285–317.

Hurford, A.J., Fitch, M. & Jäger, E. (1984) Resolution of the age structure of the detrital zircon populations of two Lower Cretaceous sandstones from the Weald of England by fission track dating. *Geol. Mag.*, **121**, 269–277.

Jaillard, E. (1997) Sintesis estratigrafica del cretaceo y paleogeno de la cuenca oriental del Ecuador. *Convenio ORSTOM-Petroproduccion*, Quito.

Jaillard, E., Benitez, S. & Mascle, G.H. (1997) Les déformations paléogènes de la zone d'avant-arc sud-équatorienne en relation avec l'évolution géodynamique. *Bull. Soc. Géol. France*, **168**, 403–412.

Jaillard, E., Ordonez, M., Jimenez, N., Suarez, J. & Toro, J. (2002a) Litho-and biostratigraphy of the Late Cretaceous-Paleogene detrital units of the Western Cordillera of Ecuador (0–4°S). 3rd Europ. Meet. Paleont. Stratigr. Latin Amer.-EMPSLA, Toulouse 2002. *Ext. Abstracts Vol.*, pp. 63–66.

Jaillard, E., Hérail, G., Monfret, T. & Wörner, G. (2002b) Andean geodynamics: main issues and contributions from the 4th ISAG, Göttingen. *Tectonophysics*, **345**, 1–15.

Kerr, A.C., Aspden, J.A., Tarney, .J. & Pilatasig, L.F. (2002) The nature and provenance of accreted oceanic terranes in western Ecuador: geochemical and tectonic constraints. *J. Geol. Soc. London*, **159**, 577–594.

Lapierre, H., Bosch, D., Dupuis, V., Polvé, M., Maury, R.C., Hernandez, J., Monié, P., Yeghicheyan, D., Jaillard, E., Tardy, M., Mercier de Lépinay, B., Mamberti, M., Desmet, A., Keller, F. & Sénebier, F. (2000) Multiple plume events in the genesis of the peri-Caribbean Cretaceous oceanic plateau province. *J. Geophys. Res.*, **105**, 8403–8421.

Litherland, M., Aspden, J.A. & Jemielita, R.A. (1994) The metamorphic belts of Ecuador. *Br. Geol. Survey Overseas Mem.*, **11**, 147 pp.

Litherland, M., Egüez, A. & Zamora, A. (1993) Mapa geológico del Ecuador, escala 1: 1 000 000. *Cogidem, BGS*, Quito.

Mange, M.A. & Maurer, H.F.W. (1992) *Heavy Minerals in Colour*. Chapman & Hall, London.

Mégard, F. (1987) Structure and evolution of the Peruvian Andes. In: *The Anatomy of Mountain Ranges* (Ed. by J.P. Schaer & J. Rodgers), pp. 179–210. Princeton University Press, Princeton, NJ, 179–210.

Moore, M.A. & England, P.C. (2001) On the inference of denudation rates from cooling ages of minerals. *Earth Planet. Sci. Lett.*, **185**, 265–284.

Naeser, C.W. (1979) Thermal history of sedimentary basins: fission-track dating of subsurface rocks. In: *Aspect of diagenesis* (Ed. by P.A. Scholle & P.R. Schluger) SEPM Spec. Publ., **26**, 109–112.

Najman, Y., Garzanti, E., Pringle, M., Bickle, M., Stix, J. & Khan, I. (2003) Early-Middle Miocene paleodrainage and tectonics in the Pakistan Himalayan: *GSA* Bull. **115**(10), 1265–1277.

Najman, Y.M.R., Pringle, M.S., Johnson, M.R.W., Robertson, A.H.F. & Wijbrans, J.R. (1997) Laser $^{40}Ar/^{39}Ar$ dating of single detrital muscovite grains from early foreland-basin sedimentary deposits in India; implications for early Himalayan evolution. *Geology*, **25**, 535–538.

Noble, D.C., McKee, E.H. & Mégard, F. (1979) Early Tertiary 'Incaic' tectonism, uplift, and volcanic activity, Andes of central Peru. *Geol. Soc. Am. Bull.*, **90**, 903–907.

Pecora, L., Jaillard, E. & Lapierre, H. (1999) Paleogene accretion and dextral displacement of an oceanic terrane in northern Peru. *C. Re.Acad. Sci.*, Paris Sér. IIa, **329**(6), 389–396.

Rivadeneira, M. & Baby, P. (1999) La Cuenca Oriente: estilo tectónico, etapas de deformación y caracteristicas geológicas de los principales campos de Petroproducción. *Convenio ORSTOM-Petroproducción*, Quito.

Romeuf, N., Aguirre, L., Soler, P., Féraud, G., Jaillard, E. & Ruffet, G. (1995) Middle Jurassic volcanism in the Northern and Central Andes. *Rev. Geol. Chile Santiago*, **22**, 245–259.

Ruiz, G. (2002) Exhumation of the northern Sub-Andean Zone of Ecuador and its source region: a combined thermochronological and heavy mineral approach. Unpublished PhD Thesis (14905), ETH, Zurich, Switzerland.

Sambridge, M.S. & Compston, W. (1994) Mixture modelling of multi-components data sets with application to ion-probe zircon ages. *Earth Planet. Sci. Lett.*, **128**, 373–390.

Sandeman, H.A., Clark, A.H. & Farrar, E. (1995) An integrated tectono-magmatic model for the evolution of the southern Peruvian Andes (13–20°S) since 55 Ma. *Intern. Geol. Rev.*, **37**, 1039–1073.

Sooms, M. (1990) Abkühlungs- und Hebungsgeschichte der Externmassive und der pennischen Decken beidseits der Simplon-Rhone-Linie seit dem Oligozän: Spaltspuringdatierungen an Apatit/Zircon und K-Ar-Datierungen an Biotit/Muskowit (Westliche Zentralalpen). Unpublished PhD Thesis, University of Bern, Switzerland.

Spiegel, C., Kuhllemann, J., Dunkl, I., Frisch, W., Von Eynatten, H. & Balogh, K. (2000) The erosion history of the Central Alps: evidence from zircon fission track data of the foreland basin sediments. *Terra Nova*, **12**, 163–170.

Spikings, R., Seward, D., Winkler, W. & Ruiz, G. (2000) Low-temperature thermochronology of the northern Cordillera Real, Ecuador: tectonic insights for zircon and apatite fission track analysis. *Tectonics*, **19**, 649–668.

Spikings, R.A., Winkler, W., Seward, D. & Handler, R. (2001) Along-strike variations in the thermal and tectonic response of the continental Ecuadorian Andes to the collision with heterogeneous oceanic crust. *Earth Planet. Sci. Lett.*, **186**, 57–73.

Steinmann, G. (1929) *Geologie von Peru* (Ed. by Karl Winter). Heidelberg.

Tagami, T., Carter, A. & Hurford, A.J. (1996) Natural long-term annealing of the zircon fission-track system in Vienna Basin deep borehole samples: constraints upon the partial annealing zone and closure temperature. *Chem. Geol.*, **130**, 147–157.

Tschopp, H.J. (1953) Oil exploration in the Oriente of Ecuador. *AAPG Bull.*, **37**, 2303–2347.

Von Eynatten, H., Gaupp, R. & Wijbrans, J.R. (1996) $^{40}Ar/^{39}Ar$ laser-probe dating of detrital white micas from Cretaceous sediments rocks of the Eastern Alps: Evidence for a Variscan high-pressure metamorphism and implications for Alpine orogeny. *Geology*, **24**, 691–694.

Wasson, T. & Sinclair, J.H. (1927) Geological Explorations East of the Andes in Ecuador. *Bull. Am. Assoc. Petrol. Geol.*, **11**, 1253–1281.

White, H.J., Skopec, R.A., Ramirez, F.A., Rodas, J.A. & Bonilla, G. (1995) Reservoir characterization of the Hollin and Napo Formations, Western Oriente Basin, Ecuador. In: *Petroleum basins of South America* (Ed. by A.J. Tankard, S.R. Suárez & H.J. Welsink) AAPG Mem., **62**, 573–596.

Willett, S.D. & Brandon, M.T. (2002) On steady states in mountain belts. *Geology*, **30**, 175–178.

Yamada, R., Tagami, T., Nishimura, S. & Ito, H. (1995) Annealing kinetics of fission-tracks in zircon: an experimental study. *Chem. Geol.*, **122**, 249–258.

Zambrano, I., Ordoñez, M. & Jiménez, N. (1999) Micropaleontologia de 63 muestras de afloramientos de la Cuenca Oriental Ecuatoriana. *Informe Tecnico No. 016-PPG-99, LABOGEO, Petroproducción,* distrito de Guayaquil.

Zeitler, P.K., Johnson, N.M., Briggs, N.D. & Naeser, C.W. (1986) Uplift history of the NW Himalaya as recorded by fission-track ages on detrital Siwalik zircons. In: *Proceedings of the Symposium on Mesozoic and Cenozoic Geology in Connection of the 60th Anniversary of the Geological Society of China* (Ed. by H. Jiqing) Geol. Publ. House, 481–496.

Manuscript received 17 December 2003; Manuscript accepted 30 June 2004

